NAP-2013

InAsSbP-based Quantum Dot Mid-Infrared Photodetectors: Fabrication, Properties and Applications

K.M. Gambaryan[1,*], V.G. Harutyunyan[1,†], V.M. Aroutiounian[1,‡],
T. Boeck[2,§], O. Marquardt[3,**], F. Schuette[2,††]

[1] *Department of Physics of Semiconductors and Microelectronics, Yerevan State University, 1 A. Manougian str., Yerevan, 0025, Armenia*
[2] *Leibniz Institute for Crystal Growth (IKZ), Max-Born-str. 2, D-12489 Berlin, Germany*
[3] *Paul Drude Institut für Festkörperelektronik (PDI), Hausvogteiplatz 5-7, 10117 Berlin, Germany*

The mid-infrared photoconductive cells (PCC) made of n-InAs(100) crystals with InAsSbP quantum dots (QDs) on the PCC surface, as well as InAsSbP-based diode heterostructures with QDs on epilayer–substrate interface are reported. Both QDs-based semiconductor structures are considered as attractive devices for several mid-infrared applications. The liquid phase epitaxy, AFM, TEM and STM techniques are utilized for the growth of QDs and epitaxial cap layers and their characterization, respectively. Anomalous photovoltaic effect is detected in PCC with type-II QDs. The open-circuit voltage and short-circuit current are measured versus radiation power density of the He-Ne laser at λ = 3.39, 1.15 and 0.63 µm wavelengths. The formation of QDs leads to the increasing of the PCC's sheet resistance up to one order and results in red shift of the photoresponse spectrum. The QDs-based PCC's voltage and current responsivity at room temperature are equal to 1.5 V/W and 82 mA/W, respectively, at zero bias and λ = 3.39 µm. The main peak at 3.48 µm and additional peaks at 2.6 µm and 2.85 µm wavelengths revealed on QDs-based devices' photoresponse and luminescence spectra allow to fabricate optical gas sensors, in particularly, for the methane, water vapor and carbon dioxide detection.

Keywords: Quantum dots, Photoconductive Cells, Diode heterostructures, Mid-Infrared.

PACS number(s): 81.05.Ea, 61.46.-w, 62.23.Eg

1. INTRODUCTION

Semiconductor quantum dots (QDs) confine electrons and holes in all three dimensions, which lead to a δ-like electronic density of states where the energy levels are totally quantized. This property is making them attractive for optoelectronic devices not only for improved laser diodes, but also for single photon sources, quantum computing systems and new generation QD-photodetectors [1, 2]. For lasers less temperature sensitive threshold current and emission wavelength, as well as longer wavelengths to mid-infrared region can be achieved. This also leads to an increase in infrared photodetectors response and operating temperature as well as photovoltaic (PV) solar cells and thermo-PV (TPV) cells efficiency [2-4]. In contrary to traditional photodiodes, photoconductive cells (PCC) can provide a very economic and technically superior solution for many applications where the presence or absence of light is just detected (digital operation) or where the intensity of light should be measured (analog operation) [5]. In photoconductive cells the bulk (or surface) resistivity decreases with increasing of the intensity of radiation allowing more photocurrent to flow. This resistive characteristic gives bulk effect photoconductors a unique quality: signal current from a detector can be varied over a wide range by adjusting the applied voltage. Such infrared sensors are valuable because they operate in the passive mode, unlike radars, which are active. Additionally, IR sensors possess the advantages of low mass and power consumption. The state-of-the-art performance of these devices makes it possible to sense several types of gaseous plumes and emissions enabling chemical warfare agent detection / discrimination.

Narrow band-gap III–V semiconductor materials like InAs, GaSb, InSb and their ternary and quaternary alloys are particularly interesting and useful since they are potentially promising to access mid- and far-infrared wavelength regions. Another alternative to direct band-gap detectors is the inter-subband transitions in quantum-confined heterostructures using III-V technology. The advantage of this quantum well infrared photodetector (QWIP) [3, 5] approach is the availability of a mature III-V fabrication technology and multi-spectral capability. These heterostructures have a narrow absorption spectrum that can be tuned by varying the quantum well width and barrier layer compositions. There is a large range of material combinations available allowing the tailoring of band-gaps through stacking of thin layers. The newest in the competition for infrared photodetector is the normal incidence

* kgambaryan@ysu.am

† harutyunyan@ysu.am

‡ aroutiounv1@yahoo.com

§ torsten.boeck@ikz-berlin.de

** marquardt@pdi-berlin.de

†† franziska.schuette@ikz-berlin.de

quantum-dot photodetectors (QDIPs) [1, 3, 5-7] in semiconductors such as InGaAs/InP, InGaAs/GaAs, InGaAs/InAs, InSb/InAs, InAsSbP/InP and SiGe/Si. These and other QDs-based devices are expected to perform well at elevated temperatures due to their three-dimensional carrier confinement characteristics. QDIPs are inherently sensitive to normal incidence IR radiation. Dark current also is much lower than that of QWIPs. This technology is useful in remote sensing, chemical and biological detection application, as well as in PV and TPV cells. Some researchers use long wavelength infrared QDIPs for spectroscopic applications. Bhattacharya et al [3] presented several heterostructure designs for obtaining improved responsibility in InGaAs/GaAlAs mid- and far-infrared QDIPs. It is noted that AlGaAs barriers when appropriately inserted in these heterostructures, can perform wonders to the design and performance improvement of the QDIPs.

Among quantum size objects' fabrication techniques, the self-organized Stranski–Krastanow (S–K) method is an important one by which dislocation-free nanostructures can be produced [8]. Depending on the growth conditions, the elastic strain can be relaxed by the formation of QDs, quantum rings or even unique island-pit pairs. For III–V compound semiconductors such as InAs, InP or InSb, one has to remark the very large difference in the respective diameters of the V element. One can therefore monitor the strain by adequate substitution between smaller/larger V element atoms. This could be used as mixed compounds such as InAsSbP, a promising candidate because it can cover the 3–5 μm mid-infrared regions adjusting its alloy composition with three V elements only. Actually, InAsSbP QDs have been successfully grown on InAs(100) substrate[9-11], while in contrast, only a few studies on quaternary QDs/nanopits nucleation have been reported so far [12, 13]. In fact, nanopits could have a different reactivity e.g. to adsorbents and could potentially be used as a mold to selectively grow specific nanostructures. Monitoring the composition ratio between As, Sb and P could lead to strain control in InAsSbP leading to nanopits formation instead of/or together with QDs.

In this paper, we report our efforts to fabricate the low bias and room temperature InAsSbP QD PCCs made of n-InAs (100) crystals, as well as n-InAs/p-InAsSbP diode heterostructure with QDs inside the p-n junction spatial charge region for several mid-infrared applications. Some structural and optoelectronic properties of those devices are presented and investigated.

2. EXPERIMENTAL PROCEDURES

Two binary substrates can be matched with InAsSbP quaternary alloy: InAs and GaSb. However, InAs substrates are used here because they are less expensive and have a higher quality compared to GaSb. The modified version of liquid phase epitaxy (LPE) is applied for both the growth of epitaxial films and for nucleation of the QDs. The samples were grown using a slide-boat crucible. In contrast to other growth techniques like molecular beam epitaxy (MBE) or metal organic chemical vapor deposition (MOCVD), LPE operates comparatively closer to thermodynamically equilibrium. To ensure a high purity of the epitaxial layers the entire growth process has performed under a pure hydrogen atmosphere. The InAs substrates used in this work were 11 mm in diameter, (100) oriented, undoped, having background electron concentration of 2×10^{16} cm^{-3}. For the growth solution formation the 7N indium, 6N antimony, undoped InAs and InP crystals were used. An atomic force (AFM), transmission electron (TEM) and scanning tunneling (STM) microscopes are used for investigation and characterization of QDs morphology, dimensions and distribution density. An infrared spectrometer (IRS-21) is used to investigate the photoresponse spectra.

3. RESULTS AND DISCUSSION

Two samples were prepared for investigations. The first sample consists of unencapsulated spherical InAsSbP type-II QDs grown on InAs(100) substrate. Second sample is a n-InAs/p-InAsSbP diode heterostructure with QDs embedded to the p-n junction spatial charge region. Either QDs or epitaxial p-InAsSbP epilayer with 4 μm of thickness were grown from a quaternary In-As-Sb-P melt by LPE with a modified slide-boat crucible at initial growth temperature of T = 550°C. According to the InAs–InSb–InP quasiternary phase diagram, as a starting point, we use the quaternary liquid phase composition that corresponds to the $InAs_{0,81}Sb_{0,06}P_{0,13}$ alloy in solid phase, that is conveniently lattice-matched to InAs substrate. QDs were grown at isothermal conditions, but the concentrations of antimony and phosphorus in the growth solution were chosen to provide a lattice mismatch up to 3% between the InAs substrate and InAsSbP wetting layer at T = 550°C. Other technological conditions and the experimental setup for the growth of QDs by LPE are described in Ref. [9-12]. Second sample was prepared by two steps, but at single technological process using two liquid phases. First, QDs were nucleated on the epi-ready substrate surface at isothermal conditions (t_1 = 10 min). Then the liquid phase was changed and the p-InAsSbP epilayer was grown by step-cooling version of LPE at ΔT = 8°C to provide 4 μm of epilayer thickness. Band-gap energy of the cap epilayer was specially chosen to be equal to ~0.48 eV at T = 78 K in order to provide both an "optical window" and localization also the electrons along with the holes inside the capsulated type-II QDs.

AFM images of the InAsSbP type-II QDs grown on InAs(100) substrate by LPE in plain and oblique views are presented in Fig. 1 (a-c). Statistical evaluation of AFM measurements shows that the areal density of QDs ranges from 6 to 8×10^9 cm^{-2}, with heights from 0.5 nm to 25 nm and widths dimensions from 10 nm to 40 nm. The QDs' number versus their average diameters (histogram) is presented in Fig. 1(d). An optimal value for the QDs diameter is equal to ~22 nm. From Fig. 1(d) it is definitely visible that the bimodal growth mode is also revealed. Additionally note that QDs size distribution is well fitted by Gram–Charlier function.
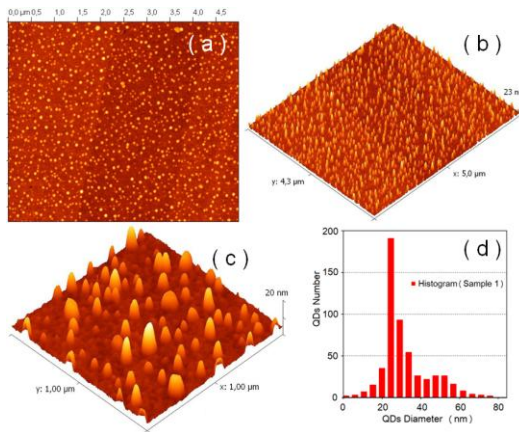
Fig. 1 – AFM images of the InAsSbP type-II QDs grown on InAs(100) substrate by LPE: (a) – plain view (S = 5×5 μm²), (b, c) – oblique views from S = 5×4.5 μm² and S = 1×1 μm², respectively. (d) – QDs histogram (Sample 1).
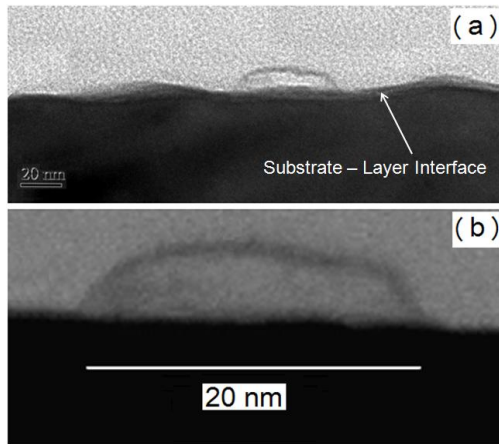

Fig. 2 – TEM image of the QDs n-InAs/p-InAsSbP diode heterostructure's cross-sectional area – (a), STM image of the single InAsSbP QD – (b)

TEM and STM investigations (Fig. 2) of the diode heterostructure's (Sample 2) cross-sectional area revealed a presence of QDs on the substrate–epilayer interface, with an average diameter and height within 10–30 nm and 3–20 nm, respectively.

The ohmic contacts to Sample 1 were formed by traditional vacuum evaporation technique in the form of Cr/Au sandwich with further thermal annealing. Geometric configuration and topology of contacts were chosen to provide uniform current flow. PCC's active surface area was equal to 10^{-2} cm². A schematic view of the InAs-based QD PCC is presented in Fig. 3. An infrared spectrometer (IRS-21) was used to investigate the photoresponse spectra of prepared device structures. The room temperature photoresponse (PR) spectra of the mid-infrared QD PCC (Sample 1) at different applied voltages are presented in Fig. 4.
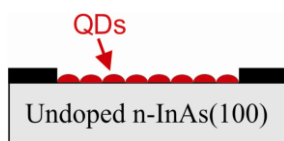

Fig. 3 – Shematic view of the InAs-based QD photoconductive cell (Sample 1)
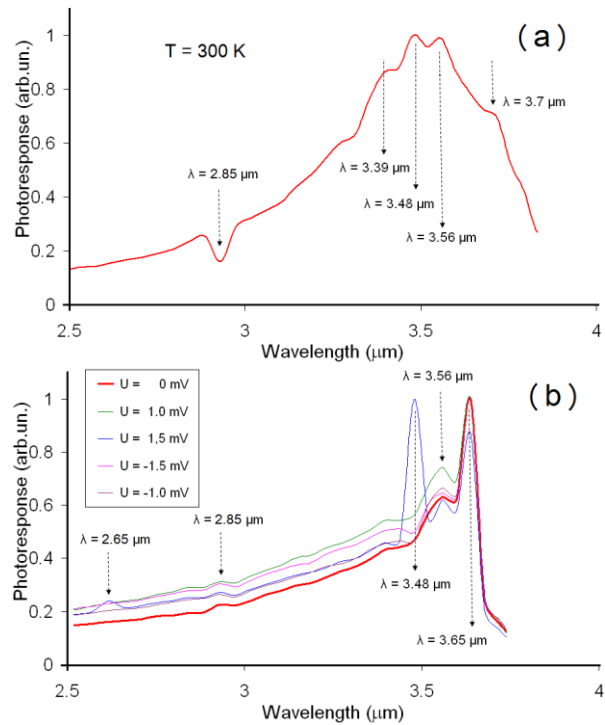

Fig. 4 – Room temperature photoresponse spectra of the mid-infrared QD PCC (Sample 1) at 2 mV – (a) and different applied voltages – (b)

As it is seen from Fig. 4, on the PR spectra of PCC with QDs are revealed not only enlargement toward the long wavelengths (a red shift) up to $\lambda = 3.7$ μm, but also additional peaks at $\lambda = 2.65$ μm, $\lambda = 2.85$ μm, $\lambda = 3.56$ μm and $\lambda = 3.65$ μm, which were not been detected on PR spectrum of InAs-based PCC without QDs. Note, that the main peak for the band-to-band transitions in InAs bulk crystals corresponds to $\lambda = 3.48$ μm at room temperature. We assume that the QDs are responsible for those additional peaks due to occured band-to-QDs subband transitions. It is seen that even at very low applied voltages (± 2 mV) a sufficient increasing of the PR signal on additional peaks is occurred. In particularly, at U = ± 1.5 mV the value of PR signal at $\lambda = 3.65$ μm becomes practically equal to the signal's value of the main maximum at $\lambda = 3.48$ μm. Our experiments also shown, that the formation of QDs leads to the increasing of the PCC's sheet resistance up to one order. These properties of the discussed QD PCCs make them very attractive, in particularly for the fabrication of multicolor mid-infrared photodetectors. Other very important features of those devices are that they can work at room temperature and that for power supply can be used even consumer accumulators and batteries. Because the most important industrial gases have a strong absorption in mid-infrared region, in particularly, methane at $\lambda = 3.3$ μm, CO_2 at 2.65 μm, as well as water vapor at $\lambda = 2.85$ μm, therefore, proposed and fabricated QD PCCs can be also used as a detectors in optical gas sensors and systems. Other very important application is determination of the glucose concentration in human blood, other biomaterials, etc.

Presence of the photoresponse signal at zero applied voltage has been also detected for the Sample 1, which is explained by the spatial separation of charge carriers in

type-II QDs and arising of the polarization potential in QDs. Obviously, this property can be applied and used in photovoltaic and thermo-photovoltaic cells and similar structures. The voltage and current maximal sensitivities of the InAsSbP type-II QDs based photodetector at cw He-Ne laser radiation with $\lambda = 3.39$ μm were equal to 2 V/W and 82 mA/W, respectively, at room temperature. Relative variation of the surface resistance of prepared mid-infrared ptotodetectors with QD versus the power density of cw He-Ne laser at different wavelengths was also measured at room temperature. The maximum drop of surface resistance at laser radiation down to 14 % for $\lambda = 1.15$ μm wavelength and 17 % for $\lambda = 3.39$ μm wavelength was detected, which is rather good result, especially for narrowband and low-resistance structures. This drop will obviously be significantly larger (up to 20%) under action of the longer wavelength radiation, taking into account that the much stronger photoresponse signal was detected at $\lambda = 3.6$ μm. Obviously, fabricated photodetectors can be used also for detecting the thermal radiation of an object heated up to 1200-1300 ⁰C temperatures.

Next, the photoluminescence (PL) spectra measurements at liquid nitrogen temperature and Fourier-transform infrared spectroscopy (FTIR) at room temperature were performed for samples 1 and 2. FTIR measurements have shown a red shift of the absorption edge for both QD devices up to 30 meV at room temperature. PL spectra of the InAs-based QD PCC (Sample 1) and n-InAs/p-InAsSbP diode heterostructure with QDs (Sample 2) at T = 78 K are presented in Fig. 5. As it is seen, for the first structure the main peak at E=0.404 eV and an additional peak at E = 0.397 eV are revealed on PL spectrum. The main peak at E = 0.404 eV coincides to the band-gap energy for the undoped InAs at liquid nitrogen temperature. An additional peak at E = 0.397 eV is explained by the direct radiative recombination already occurred inside the QD, because, theoretical calculations show [13] that in InAsSbP-based QD structures, however, due to a shallow barrier a weak localization of electrons is also possible. This localization allows electrons to recombine with the holes inside QDs before pushed out to the InAs matrix.

In Sample 2 p-type cap layer creates an additional potential barrier for the exited electrons and the probability of direct radiative recombination inside the QDs sufficiently increases, which is confirmed by the strong peak appeared on PL spectrum at E = 0.371 eV and red-shifted from the main peak up to 33.2 meV. A specific fractures on the Sample 2 PL spectrum are also visible at E = 0.382

eV, E = 0.39 eV and E = 0.398 eV, which are not appeared on the unencapsulated QDs' PL spectrum (Sample 1). We suggest that these fractures are not an experimental artifact and correspond to holes exited states.
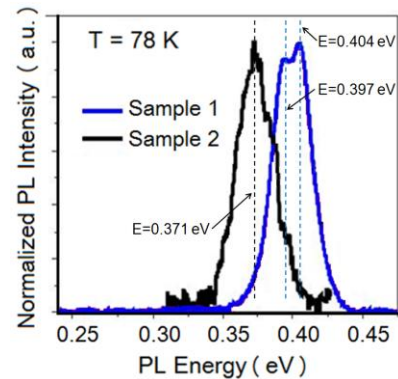

Fig. 5 – Photoluminescence spectra of the InAs-based QD PCC (Sample 1) and n-InAs/p-InAsSbP diode heterostructure with QDs (Sample 2) at T = 78 K

4. CONCLUSIONS

Thus, the mid-infrared photoconductive cells made of n-InAs(100) crystals with InAsSbP QDs on the PCC surface, as well as InAsSbP-based diode heterostructures with QDs on epilayer–substrate interface were fabricated and investigated. Both QDs-based semiconductor structures are considered as attractive devices for several mid-infrared applications. The photovoltaic effect was detected in PCC with type-II QDs. The open-circuit voltage and short-circuit current are measured versus radiation power density of the He-Ne laser at $\lambda = 3.39$, 1.15 and 0.63 μm wavelengths. The formation of QDs leads to the increasing of the PCC's sheet resistance up to one order and results in red shift of the photoresponse spectrum. The QDs-based PCC's voltage and current responsivity at room temperature are equal to 1.5 V/W and 82 mA/W, respectively, at zero bias and $\lambda = 3.39$ μm. The main peak at 3.48 μm and additional peaks at 2.6 μm and 2.85 wavelengths revealed on QDs-based devices' photoresponse and PL spectra allow fabricating optical gas sensors for the methane, water vapor and carbon dioxide detection, determination of the glucose concentration in human blood, as well as for other very important mid-infrared applications.

REFERENCES

1. D. Bimberg, M. Grundmann, N.N. Ledentsov, *Quantum Dot Heterostructures* (New York: Wiley: 1998).
2. J. Wu, D. Shao, V.G. Dorogan, A.Z. Li, S. Li, E. A. DeCuir, Jr., M.O. Manasreh, Z.M. Wang, Y.I. Mazur, G.J. Salamo, *Nano Lett.* **10**, 1512 (2010).
3. P. Bhattacharya, X.H. Su, S. Chakrabarti, G. Ariyawansa, A.G.U. Perera, *Appl. Phys. Lett.* **86**, 191106 (2005).
4. J. Wu, Y.F.M. Makableh, R. Vasan, M.O. Manasreh, B. Liang, C.J. Reyner, D.L. Huffaker, *Appl. Phys. Lett.* **100**, 051907 (2012).
5. A. Rogalski, *Acta Physica Polonica A* **116**, 389 (2009).
6. X. Lu, J. Vaillancourt, M.J. Meisner, A. Stintz, *J. Phys. D: Appl. Phys.* **40**, 5878 (2007).

7. K.M. Gambaryan, V.M. Aroutiounian, V.G. Harutyunyan, *Infrared Phys. & Technol.* **54**, 114 (2011).
8. I. Stranski, L. Krastanow, Math.-Naturwiss. **146**, 797 (1938).
9. K.M. Gambaryan, V.M. Aroutiounian, T. Boeck, M. Schulze, P.G. Soukiassian, *J. Phys. D: Appl. Phys.* **41**, 162004 (2008).
10. K.M. Gambaryan, V.M. Aroutiounian, V.G. Harutyunyan, O. Marquardt, P.G. Soukiassian, *Appl. Phys. Lett.* **100**, 033104 (2012).
11. K.M. Gambaryan, V.M. Aroutiounian, V.G. Harutyunyan, *Appl. Phys. Lett.* **101,** 093103 (2012).
12. K.M. Gambaryan, Nanoscale Res. Lett. 5, 587 (2010).
13. O. Marquardt, T. Hickel, J. Neugebauer, K.M. Gambaryan, V.M. Aroutiounian, *J. of Appl. Phys.* **110,** 043708 (2011).